

## THERMAL FOULING OF HEAT EXCHANGER TUBES DUE TO HEAVY HYDROCARBON DROPLETS IMPINGEMENT

P. Verhees, A.V. Mahulkar, K. M. Van Geem and G.J. Heynderickx\*

Laboratory for Chemical Technology, Ghent University, Technologiepark 914, B-9052 Zwijnaarde, Belgium

\*: corresponding author: geraldine.heynderickx@ugent.be

### ABSTRACT

This work discusses fouling in the vapor-steam mixture overheater in the convection section of an industrial steam cracker due to the thermal degradation of heavy hydrocarbon droplets deposited on the tube wall. A *spray* of heavy hydrocarbon multi-component droplets is injected in a tube of the vapor-steam mixture overheater and the path of the droplets through the tube is followed by an Eulerian-Lagrangian CFD simulation. To study tube fouling the droplet impingement behavior on the wall, the evaporation of the deposited liquid and a coking model describing thermal coke formation due to degradation of heavy hydrocarbons are required. To describe the droplet impingement behavior a regime map for single component millimeter-sized droplets is taken from literature. Two simulations are performed to study fouling problems in a vapor-mixture overheater tube. Simulation results are found to be grid sensitive. By analyzing and comparing simulation results it is concluded that reliable fouling data require a regime map for the impingement of multi component heavy hydrocarbon micron-sized droplets.

### INTRODUCTION

Droplet impingement is extremely important in many applications, e.g. in internal combustion engines (Ogawa et al., 1997), spray coating (Werner et al., 2007), spray drying and cooling (Horacek et al., 2005), etc. Depending on the application droplets are preferred to stick, rebound or splash.

Research on droplet impingement in heat exchanger tubes in the convection section of a steam cracker (Fig. 1) has recently gained attention (Mahulkar et al., 2012, 2014, 2015). Fouling of heat exchanger tubes in the steam cracker convection section is found to increase due to the use of heavier hydrocarbon feedstocks. Incomplete evaporation of the feed results in a spray of heavy hydrocarbon micron-sized droplets entering the tubes of the vapor-steam mixture overheater tubes in the steam cracker convection section, resulting in coke formation on the tube walls. A discussion of the different heat exchangers in a steam cracker convection section is found in De Schepper et al. (2009b). To accurately describe tube fouling in the vapor-steam mixture overheater tube in the convection section of a steam cracker, the droplet-wall interaction upon impingement

needs to be understood and described. The interaction is governed by forces (inertia, surface tension, viscous forces and adhesion) that depend in turn on droplet properties (density, diameter, velocity, surface tension, viscosity, boiling point) and wall properties (temperature, roughness, contact angle). Balancing the forces allows determining the impact behavior as function of the wall temperature and the (normal impact) Weber number (Mahulkar et al., 2015). The impingement behavior is presented in so-called regime maps, predicting the impact behavior as a function of Weber number and wall temperature.

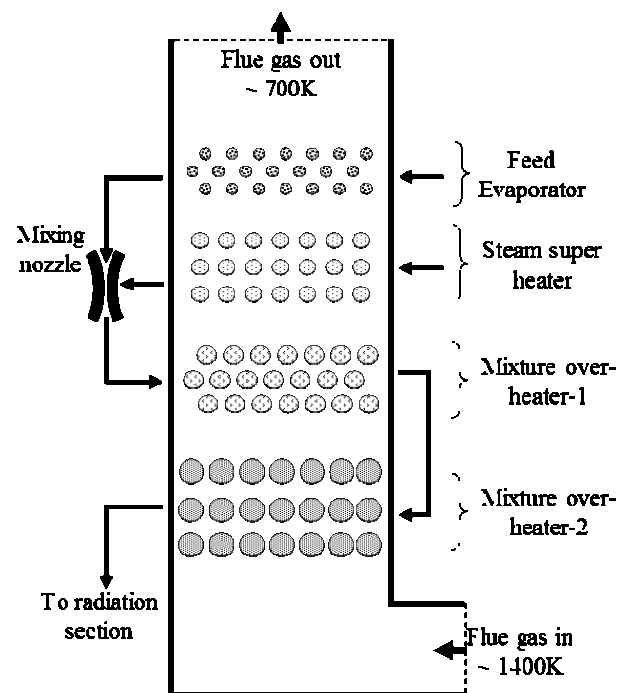


Fig. 1: Steam cracker convection section (Mahulkar et al., 2014)

Regime maps have been constructed, based on experimental data, by Bai and Gosman (1995); Grover and Assanis (2001) and Lee and Ryu (2006), presented in Fig. 2a,b. For a detailed discussion reference is made to Mahulkar et al. (2015). These regime maps were constructed for single components with droplet sizes of the

order of millimeters. Regime maps as found in literature (Fig. 2a,b) are constructed accounting for the normal impact Weber number on the one hand and the wall temperature  $T_w$  on the other hand. The Weber number is calculated as:

$$We_{norm,in} = \frac{d v_{norm,in}^2 \rho}{\sigma} \quad (1)$$

Mahulkar et al. (2012) applied a regime map, combined with an evaporation model (De Schepper et al., 2009a) and a coking model (Wiehe, 1993) to determine fouling of vapor-steam mixture overheater tubes in the convection section of a steam cracker using a coarse simulation grid. The use of a more refined simulation grid was found to considerably alter the simulation results (Mahulkar et al., 2014).

In the presented work these simulation results are analyzed and compared. Based on this study it is concluded that regime maps as available in literature are insufficient to make a reliable simulation of fouling in a convection section steam-hydrocarbon mixture overheater tube. Regime maps for multi component heavy hydrocarbon micron-sized droplets need to be developed.

## MODELING

Fouling is due to a spray of heavy hydrocarbon droplets entering the vapor-steam mixture overheater tubes. In the present work CFD simulations are performed with ANSYS FLUENT 13.0 using the Finite Volume approach to solve the basic set of continuity equations (mass, momentum, energy, species conservation) combined with the  $k-\epsilon$  turbulence model (Lauder and Spalding, 1974) (Table 1). The *spray* behavior is simulated with an Eulerian-Lagrangian approach. A Lagrangian approach implies that the path of each spray droplet is followed in the tube (Table 1). Evaporation of the droplet in the vapor phase is accounted for. During droplet impingement, liquid can be deposited on the wall resulting in thermal degradation of the deposited heavy hydrocarbons liquid into coke.

Mahulkar et al. (2012, 2014) applied a regime map (Fig. 2c) based on the regime map developed by Lee and Ryu (Fig. 2b) to study the fouling of the mixture overheater-1 tubes (Fig. 1). The transfer to the splash behavior is observed at a critical value of the normal impact Weber Number  $We_{norm}^{crit}$  (Fig. 2a). Bai et al. (2002) developed a correlation to calculate this critical normal impact Weber number:

$$We_{norm,in}^{crit} = 1322. \left( \frac{\rho \sigma d}{\mu^2} \right)^{-0.183} \quad (2)$$

Grover and Assanis (2001) presented a splash model where the mother droplet partially sticks to the wall and three daughter droplets rebound from the wall, the Rebound with breakup region in Figure 2c. Bai et al. (2002) present a model where more than three daughter droplets are formed, the Splash region in Fig. 2c. The number of splashed droplets is calculated from:

$$N_s = 5 \left( \frac{We_{norm,in}}{We_{norm,in}^{crit}} - 1 \right) \quad (3)$$

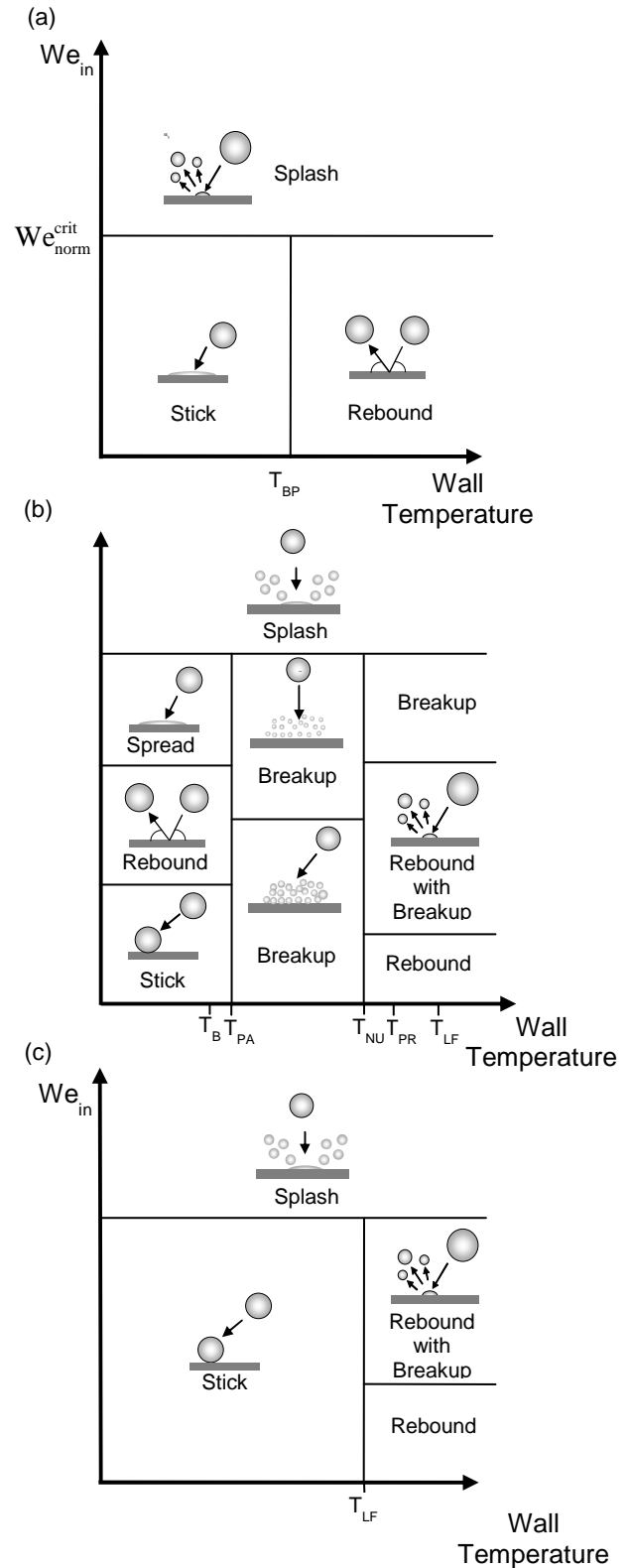


Fig. 2: Regime maps for droplet wall interaction from (a) Grover and Assanis (2001), (b) Lee and Ryu (2006) based on a modified regime map of Bai and Gosman (1995) and (c) Applied in Mahulkar et al. (2014).

Table 1: Mass, Species, momentum, energy balance equation and turbulence model equations

Mass balance	(a)
$\frac{\partial}{\partial t}(\rho) + \nabla \cdot (\rho \vec{u}) = \sum_j S_{M,j}$	
Species mass balance	(b)
$\frac{\partial}{\partial t}(\rho Y_j) + \nabla \cdot (\rho \vec{u} Y_j) = -\nabla \cdot \left[ \left( \rho D_{j,m} + \frac{\mu_t}{0.7} \right) \nabla Y_j \right] + S_{M,j}$	
Momentum balance	(c)
$\frac{\partial}{\partial t}(\rho \bar{u}_i) + \nabla \cdot (\rho \vec{u} \bar{u}) = -\nabla P + \nabla \cdot \left[ \mu \left( \nabla \vec{u} + \nabla \vec{u}^T - \frac{2}{3} \nabla \cdot \vec{u} \bar{I} \right) \right] + \nabla \cdot (\rho \vec{u}' \vec{u}') + \rho g_i + S_{F,i}$	
Energy balance	(d)
$\frac{\partial}{\partial t}(\rho E) + \nabla \cdot (\rho \vec{u} E) = \nabla \cdot \left[ (K + K_t) \nabla T - \sum_j C_{p,j} T \vec{J}_j \right] + S_E$	
$E = \sum_j Y_j \left( \int_{T_{ref}}^T C_{p,j} dT \right) + \frac{P}{\rho}$	(e)
Turbulence model	(f)
Turbulent kinetic energy balance	
$\frac{\partial}{\partial t}(\rho k) + \nabla \cdot (\rho \vec{u} k) = \nabla \cdot \left[ \left( \mu + 0.09 \rho \frac{k^2}{\varepsilon} \right) \nabla k \right] + G_k + G_b - \rho \varepsilon$	
Turbulent energy dissipation rate balance	(g)
$\frac{\partial}{\partial t}(\rho \varepsilon) + \nabla \cdot (\rho \vec{u} \varepsilon) = \nabla \cdot \left[ \left( \mu + \frac{\mu_t}{1.3} \right) \nabla \varepsilon \right] + 1.44 \frac{\varepsilon}{k} (G_k + C3G_b) - 1.92 \rho \frac{\varepsilon^2}{k}$	
Force balance over the particle	(h)
$\frac{du_{d,i}}{dt} = \frac{18\mu}{\rho_d d_d^2} \cdot \frac{C_D}{24} \cdot \frac{\rho d_d  u_i - u_{d,i} }{\mu} \cdot (u_i - u_{d,i}) + \frac{g_i (\rho_d - \rho)}{\rho_d}$	
Particle positioning	(i)
$\frac{dx_{d,i}}{dt} = u_{d,i}$	
Momentum source term for the continuous phase due to the presence of the dispersed phase	(j)
$S_{F,i} = \sum_0^{t_c} \left[ \left[ \frac{18\mu}{\rho_d d_d^2} \cdot \frac{C_D}{24} \cdot \frac{\rho d_d  u_i - u_{d,i} }{\mu} \cdot (u_i - u_{d,i}) \right] \frac{m_d}{m_{d,0}} \dot{m}_{d,0} \cdot \Delta t \right]$	
Energy source term for the continuous phase due to the presence of the dispersed phase	(k)
$S_E = \frac{m_{d,in}}{m_{d,0}} \dot{m}_{d,0} \sum_j Y_j \left( \int_{T_{ref}}^{T_{d,in}} C_{p,j} dT \right) - \frac{m_{d,out}}{m_{d,0}} \dot{m}_{d,0} \sum_j Y_j \left( \int_{T_{ref}}^{T_{d,out}} C_{p,j} dT \right) - \frac{\Delta m_d}{m_{d,0}} \dot{m}_{d,0} \sum_j Y_j h_{fg,j}$	
Mass source term for the continuous phase due to the presence of the dispersed phase	(l)
$S_M = \frac{\Delta m_d}{m_{d,0}} \dot{m}_{d,0}$	
$\Delta m_d = \sum_j \left[ k_c \left( \frac{x_j P_{sat}(T_d)}{RT_d} - \frac{Y_j P}{RT_\infty} \right) 4\pi d_d^2 \cdot t_c \right]$	(m)

The normal velocity at which the daughter droplets are rebounded in the tube is calculated using the correlation of Mundo et al. (1995) for the normal outgoing We number:

$$We_{norm,out} = 0.6785 We_{norm,in} \exp(-0.04415 We_{norm,in}) \quad (4)$$

The tangential velocity of the droplet remains unchanged. A detailed discussion of these splashing models was given by Mahulkar et al. (2014).

The heavy hydrocarbon liquid deposited on the wall is partially evaporated. An evaporation model will allow to determine the fraction of liquid that is evaporated. Evaporation/condensation of the liquid on the wall is calculated using the model applied by De Schepper et al. (2009a).

Evaporation rate:

$$m_{lv} = \gamma \alpha_l \rho_l \frac{T - T_{sat}}{T_{sat}} (T \rangle T_{sat}) \quad (5)$$

Condensation rate:

$$m_{vl} = \gamma \alpha_v \rho_v \frac{T_{sat} - T}{T_{sat}} (T \langle T_{sat}) \quad (6)$$

This model was explained in great detail by De Schepper et al. (2009a).

The non-evaporated liquid hydrocarbons on the tube wall will foul the tube due to thermal degradation resulting in coke formation. The coking rate is calculated using the kinetic model of Wiehe (1993). Basically this model accounts for evaporation of the volatile components in the deposited liquid. The non-volatile components are split into toluene-soluble components, heptane-soluble components, and asphaltenes. Asphaltenes are the main precursors of coke in the coking model of Wiehe (1993). A more detailed description of the coking model and its application to calculate the fouling of the vapor-steam mixture overheater-1 tubes by thermal degradation of deposited heavy hydrocarbon droplets was given by Mahulkar et al. (2014).

## SIMULATION

A gas chromatographic analysis (GC\*GC) of a gas condensate feed is performed. Out of the 120 components 11 reference components are selected to represent the boiling point curve (Fig. 3).

In a study by De Schepper et al. (2009a) it was determined that 70 wt% of the heavy hydrocarbon feed is evaporated in the feed evaporator (Fig. 1) of the steam cracker convection section. Mahulkar et al. (2012, 2014) calculated that another 16 wt% is evaporated in the mixing nozzle (Fig. 1) by contacting the partially evaporated feed with overheated steam (coming from the steam superheater, Fig. 1). The non-evaporated liquid, the most heavy components from the feed (Fig. 3), leaves the mixing nozzle as a spray flow. The inlet conditions for the spray in the tubes of vapor-steam mixture overheater-1 (Fig. 1) are thus determined. A mean droplet diameter of ~100 micron is calculated based on the correlation proposed by Andreussi and Azzopardi (1983).

The fouling of heat exchangers tubes in the convection section of a steam cracker is studied, by performing an

Eulerian-Lagrangian simulation for a *spray* of droplets. This spray of heavy hydrocarbon multi-component droplets with a diameter of 100 micron is injected in the bended inlet of a vapor-steam mixture overheater-1 tube (Fig. 4). The tubes of the vapor-steam mixture overheater-1 in an industrial steam cracker (De Schepper et al., 2010) have a diameter of 0.077 m, make 3 passes through the convection section (Fig. 1) and each pass is 11 m long. Mahulkar et al. (2012) constructed a 3-dimensional coarse grid in the tube with a total of 0.83 million grid cells over the complete tube length. To present the simulation results, the tube was divided in a number of zones, as presented in Fig. 4a. A grid sensitivity analysis was performed by Mahulkar et al. (2014), refining the grid to a total of 1.7 million grid cells. Grid refinement was mainly limited to those zones in the tube that were found to be sensitive to coke formation. To present the results, the tube was divided into a number of zones (Fig. 4b). More zones were chosen in the tube zones sensitive to fouling.

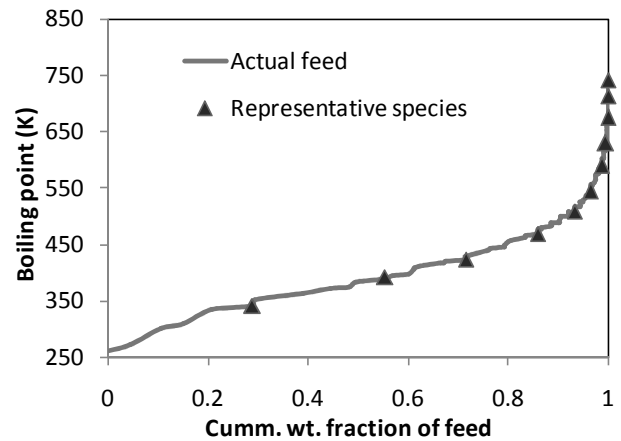


Fig. 3: Boiling point curve of gas condensate feed (Mahulkar et al., 2014)

Statistically relevant droplet trajectories are obtained by injecting a spray of 6,000 droplets, and by repeating each simulation 10 times. Simulations are performed for wall temperatures of 650 K, 700 K and 750 K. The latter temperatures are representative for a mixture-overheater-1 tube as presented by De Schepper et al. (2009b).

## RESULTS AND DISCUSSION

Upon impingement on the wall of the bended tube inlet, the normal impact We numbers (~1000) (Eq. 1) are considerably larger than the critical We number (~500) (Eq. 2). Splashing with wall stick (Fig. 2c) and the formation of multiple droplets (Eq. 3) is observed. Part of the injected liquid is deposited on the non-heated (adiabatic) wall of the bended inlet. Daughter droplets are rebounded in the tube. The trajectory of these daughter droplets through the tube is followed in the simulation. It should be mentioned that the diameter of these daughter droplets is considerably smaller than 100 micron. Thus, for each daughter droplet, the impingement model equations needs to be re-evaluated. For

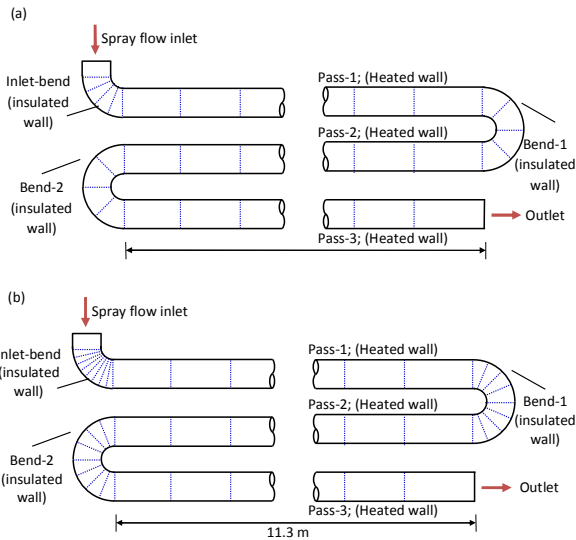


Fig. 4: Vapor-steam mixture overheater-1 tube geometry with (a) coarse grid and zoning (Mahulkar et al. (2012) and (b) fine grid and zoning Mahulkar et al. (2014)

each droplet, (partial) evaporation while flowing *through* the tube is accounted for. Droplet trajectories and the reduction of the droplet diameters in the inlet bend of the mixture overheater are presented in Fig. 5. The amount of liquid hydrocarbons deposited on the wall is then used to determine the amount of coke formed on the different zones in the tube, considering partial evaporation of the deposited liquid (Eq. 5 and Eq. 6) (De Schepper et al., 2009a), and using the coking model of Wiehe (1993).

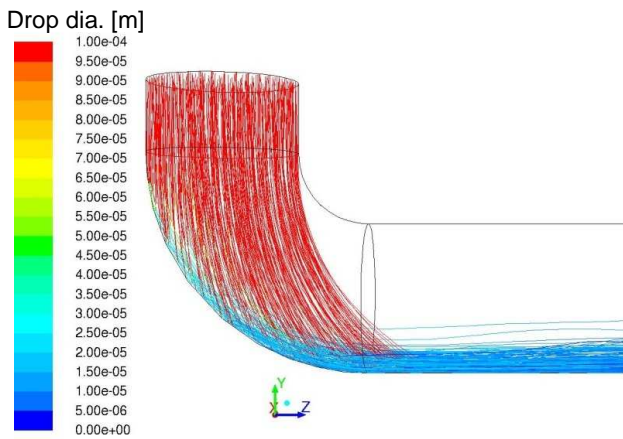


Fig.5: Droplet trajectories for 100 micron droplet (Mahulkar et al, 2014)

In Fig. 6 the liquid deposited in the different zones (Fig. 4a) of the tube is presented for the 3 wall temperatures (650 K, 700 K, 750 K) and a droplet diameter of 100 micron, as simulated by Mahulkar et al. (2012). The highest fraction of the injected liquid is deposited in the bended inlet tube (+/- 1 wt%). The 100 micron mother droplets do not follow the vapor flow lines and impinge on the tube wall. The smaller daughter droplets will follow the straight vapor lines in tube pass-1 more easily, and deposition is

low. In the U-bend, following the vapor steam lines is less obvious, even for smaller droplets, and deposition slightly rises. At the highest wall temperature no liquid is deposited in the U-bend or tube pass-2. The latter is easily explained by the fact that (partial) droplet evaporation in the tube is accounted for in the modeling. This evaporation increases with increasing wall and thus vapor temperature. Remark that, for all temperatures, the sum of deposited liquid is far from 100% of the injected liquid, due to this droplet evaporation in the vapor tube flow.

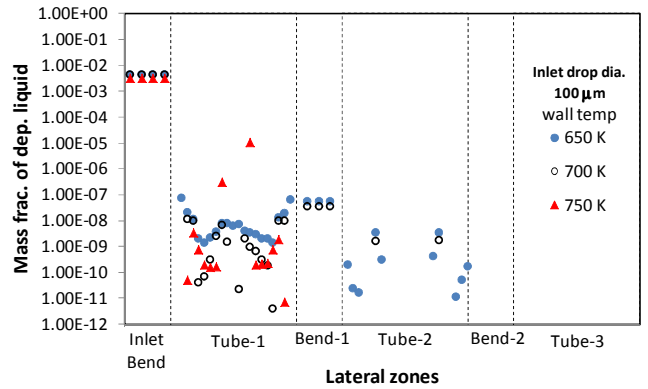


Fig.6: Mass fraction of incoming liquid deposited on tube wall (Mahulkar et al., 2012)

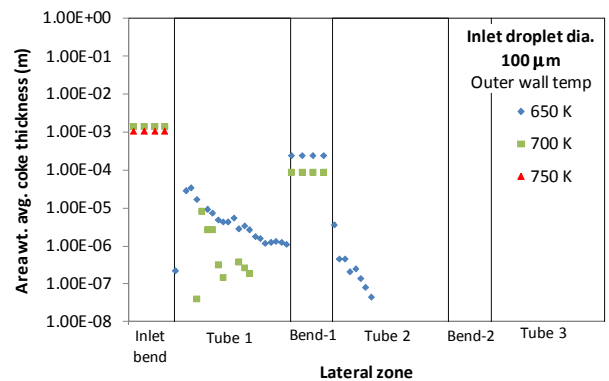


Fig. 7: Coke layer thickness following 30 days of operation (Mahulkar et al., 2012)

If a constant coking rate over 30 days is considered the coke layer thickness corresponding to Fig. 6 is presented in Fig. 7.

Some remarkable observations are made. The deposited liquid in the (non-heated) inlet bend is  $10^4$  to  $10^7$  times higher than the liquid deposited in tube pass-1. The difference in coke layer height however is considerably smaller. The latter is due to the fact that the liquid deposited in the inlet bend contains volatiles that will evaporate, even on the adiabatic wall. The liquid deposited in tube pass-1 (Fig. 4) however is rich in non-volatiles. The evaporation of these liquid deposits is limited. Furthermore, there is no coke layer on the wall of tube pass-1 if the tube wall temperature is 750 K (Fig. 7), although liquid is deposited (Fig. 6). The latter is due to the fact that all hydrocarbons have a boiling temperature below 750 K (Fig. 3) and will thus evaporate on the tube wall.

Following the thick coke layer in the bended tube inlet and the first U-bend of the tube, Mahulkar et al. (2014) decided to perform a tube simulation with considerable grid refinement in the bended tube inlet and the first U-bend of the tube.

Simulation results for liquid deposition on the tube wall when injecting 100 micron droplets in tubes with wall temperatures of 650 K, 700 K and 750 K are presented in Fig. 8 (Mahulkar et al., 2014). When comparing Fig. 6 (coarse grid and zoning) and Fig. 8 (finer grid and zoning), remarkable differences are observed. The fraction of liquid

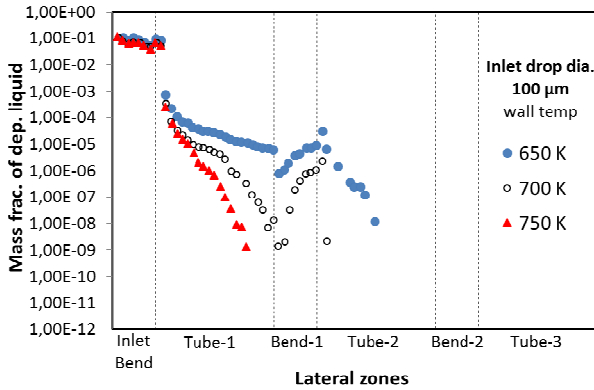


Fig. 8: Mass fraction of incoming liquid deposited on tube wall (Mahulkar et al., 2014)

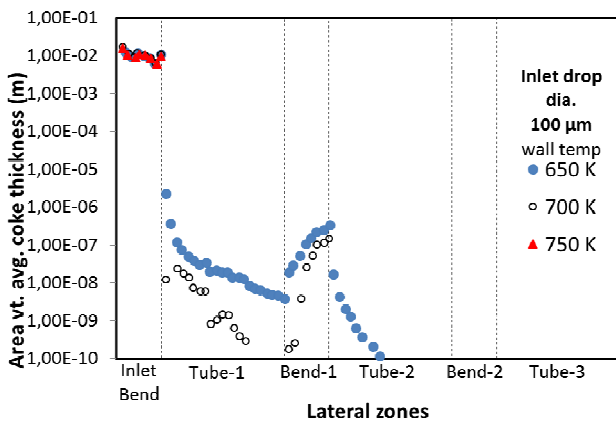


Fig. 9: Coke layer thickness following 30 days of operation (Mahulkar et al., 2014)

deposited in the inlet bend is more than 10 times higher when using a finer grid. Furthermore, liquid deposit is no longer constant over the complete tube inlet bend, but reduces with increasing length. A comparable decrease is observed in tube pass-1. However, in the first U-bend, there is a strong rise in liquid deposit while moving through the bend, while the calculated deposits in the U-bend are found to be constant with the coarse grid (Fig. 6). All these observations are explained by the fact that in the finer grid, the droplet trajectories (Fig. 5) are reconstructed in more detail, resulting in variations in liquid deposition. Indeed, while flowing through the U-bend droplets will have increasing difficulty to follow the vapor flow.

If a constant coking rate over 30 days is considered the coke layer thickness corresponding to the liquid deposit in Fig. 8 is presented in Fig. 9. Higher liquid deposits in the bended tube inlet results in a coke layer thickness of 0.01m. These results do not correspond with data provided by an industrial partner in this project (data not available for publication).

The evaporation model of De Schepper et al. (2009a) was proven to be reliable (De Schepper et al., 2009a). The thick coke layer in the bended tube inlet is thus due to the high liquid deposits in the bended tube inlet. The liquid deposits are determined based on the regime map (Fig. 2c) and the models applied to determine splashing, deposit and formation of daughter droplets (Bai and Gosman, 1995, Grover and Assanis, 2001, Bai et al., 2005) as explained above and discussed in more detail by Mahulkar et al. (2014).

Mahulkar et al. (2015) constructed regime maps based on CFD simulations of droplet impingement behavior on a hot wall. The CFD-constructed regime map for 100 micron droplet impingement is shown in Fig. 10. Snapshots of the droplet impingement behavior upon Splashing with ring formation (Splash-R) are presented in Fig. 11 (Mahulkar et al., 2015). The correlation of Bai et al. (2002) to calculate the critical We number (Eq. 2) was found to be adequate for the heavy hydrocarbon droplets of micron size. The correlation of Bai et al. (2002) to determine the number of splashed daughter droplets (Eq. 3) was found to seriously under-estimate the number of splashed droplets (Mahulkar et al., 2015). More splashed droplets upon the first impact of a 100 micron droplet result in considerably smaller daughter droplets. In turn, these droplets will have low(er) We numbers upon their impact and will most probably rebound from the hot tube wall (Fig. 2c). Furthermore, smaller droplets will evaporate more in the vapor flow, again resulting in less liquid deposits on the tube wall. Based on these considerations, tube fouling simulations are currently performed with the model developed by Mahulkar et al. (2015), replacing the model of Bai et al. (2002). Simulation results will be reported soon.

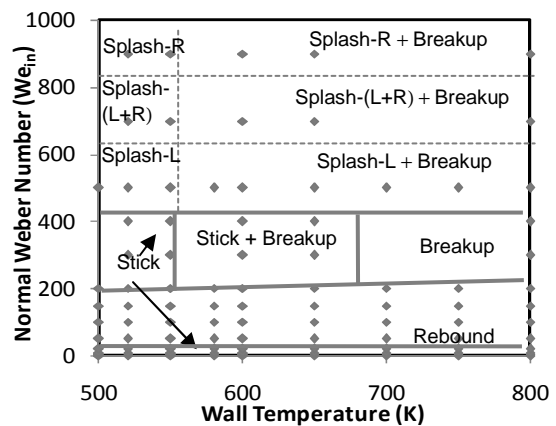


Fig. 10: Regime maps obtained from CFD simulations for heavy hydrocarbon multi-component droplet impingement for droplet diameter of 100 micron (Mahulkar et al, 2015)

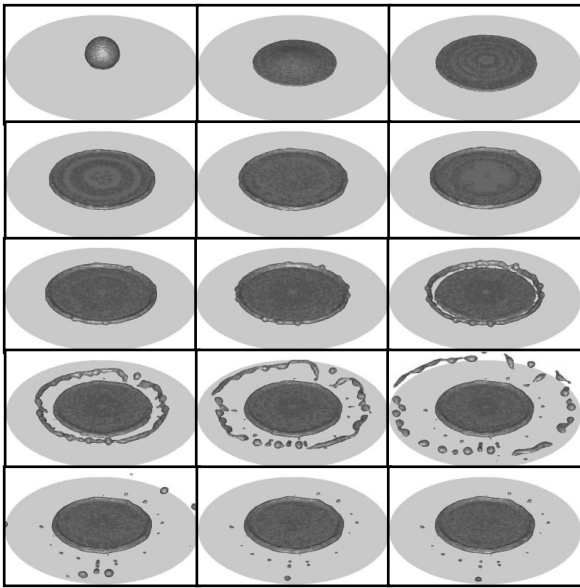


Fig. 11: Timed snapshots of Splash-R ( $We_{in}=900$ ;  $T_w=500$  K; time interval in each frame  $3\mu s$ ) (Mahulkar et al., 2015)

## CONCLUSIONS

Due to heavy hydrocarbon droplet impingement on heated tube walls liquid is deposited in the convection section heat exchangers when cracking heavy petroleum fractions. The deposited liquid hydrocarbons partially evaporate and partially undergo thermal degradation resulting in the formation of a coke layer on the tube wall. A Eulerian-Lagrangian simulation of a *spray* of heavy hydrocarbon multi-component droplets entering the tube of a vapor-steam mixture overheater tube in an industrial steam cracking convection section is performed accounting for a droplet impingement regime map and model (Bai et al. (2002), an evaporation model (De Schepper et al., 2009a) and a kinetic model for coke formation by thermal degradation of deposited heavy hydrocarbons (Wiehe, 1993). Tube fouling is simulated using two tube grids, with grid refinement in the tube sections sensitive to coke formation. From the results it is concluded that regime maps taken from literature, developed for single component millimeter-sized droplets cannot be applied to describe impingement of multi component micron-sized droplets. Regime maps are generated based on CFD simulations of droplet impact behavior (Mahulkar et al., 2015). Fouling calculations using the new impingement regime maps and models are to be reported.

## NOMENCLATURE

$C_D$  : Drag coefficient  
 $C_P$  : Specific heat (J/kg.K)  
 $d$  : Diameter (m)  
 $D$  : Diffusion coefficient ( $m^2/s$ )  
 $E$  : Total energy (J/kg)  
 $G$  : Generation of turbulence kinetic energy ( $kg/m.s^3$ )

$g$  : Gravitational acceleration ( $m/s^2$ )  
 $h_{fg}$  : Heat of evaporation of species (J/kg)  
 $I$  : Unit tensor  
 $J$  : Diffusion flux ( $kg/m^2.s$ )  
 $K$  : Thermal conductivity (J/m.K.s)  
 $k$  : Turbulent kinetic energy ( $m^2/s^2$ )  
 $m$  : Rate ( $kg/m^3/s$ )  
 $N_S$  : Number of splashed daughter droplets  
 $P$  : Pressure (Pa)  
 $S$  : Source term  
 $T$  : Temperature (K)  
 $t$  : Time (s)  
 $t_c$  : Time spent by droplet in control volume (s)  
 $u$  : Instantaneous velocity (m/s)  
 $v$  : Velocity of droplet normal to the wall (m/s)  
 $We$  : Normal Weber number ( $\rho v^2 d / \sigma$ )  
 $x$  : ordinate  
 $Y$  : Species mass fraction  
 $\gamma$  : Coefficient in phase change model (1/s)  
 $\epsilon$  : Dissipation of turbulent kinetic energy ( $m^2/s^3$ )  
 $\rho$  : Density ( $kg/m^3$ )  
 $\alpha$  : Volume fraction  
 $\sigma$  : Surface tension (N/m)  
 $\mu$  : Viscosity (Pa.s)

## Subscript

BP : Boiling point  
 $d$  : Droplet  
 $E$  : Energy  
 $i$  :  $i_{in}$  coordinate  
 $in$  : Impinging  
 $j$  : Species index in droplet  
 $l$  : Liquid  
 $m$  : Species index in continuous phase  
 $Mass$  : Mass  
 $PA$  : Pure adhesion  
 $sat$  : Saturation  
 $t$  : Turbulent  
 $v$  : Vapor  
 $w$  : Wall  
 $0$  : initial (at time 0 s)

## ACKNOWLEDGMENTS

A. Mahulkar and G.J. Heynderickx acknowledge financial support from the Fund for Scientific Research Flanders (FWO-N) for the coke formation research under project number 3.G.0022.09. This work was carried out using the Stevin Supercomputer Infrastructure at Ghent University, funded by Ghent University, the Hercules Foundation and the Flemish Government – department EWI. Authors acknowledge the 'Long Term Structural Methusalem Funding by the Flemish Government'.

## REFERENCES

Andreussi, P., Azzopardi, B.J., 1983. Droplet Deposition and Interchange in Annular 2-Phase Flow, *International Journal of Multiphase Flow*, vol. 9, pp. 681-695.  
 ANSYS, I., 2010. ANSYS FLUENT 13.0 Theory Guide Turbulence. ANSYS, Inc, PA, USA, p. 91.

- Bai, C., Gosman, A.D., 1995. Development of Methodology for Spray Impingement Simulation, *International Congress & Exposition*, February 27, Detroit, Michigan, United States, p. 75.
- De Schepper, S.C.K., Heynderickx, G.J., Marin, G.B., 2009a, Modeling the Evaporation in the Convection Section of a Steam Cracker, *Computers and Chemical Engineering*, vol. 32, pp. 122-132.
- De Schepper, S.C.K., Heynderickx, G.J., Marin, G.B., 2009b, Coupled Simulation of the Flue Gas and Process Gas Side of a Steam Cracker Convection Section, *American Institute of Chemical Engineers Journal*, vol. 32, pp. 122-132.
- De Schepper, S.C.K., Heynderickx, G.J., Marin, G.B., 2010, Modeling the Coke Formation in the Convection Section Tubes of a Steam Cracker, *Industrial & Engineering Chemistry Research*, vol. 55(11), pp. 2773-2787
- Grover, O.R., Assanis, D.N., 2001, A spray wall impingement model based upon conservation principles, The Fifth International Symposium on Diagnostics and Modeling of Combustion in Internal Combustion Engines (COMODIA 2001), Nagoya, Japan.
- Horacek, B., Kiger K., Kim J., 2005. Single nozzle spray cooling heat transfer mechanisms. *International Journal of Heat and Mass Transfer*, vol. 48, 1425-1438.
- Lauder, B.E., Spalding, D.B., 1974, The numerical computation of turbulent flows, *Computer Methods in Applied Mechanics and Engineering*, vol. 3 (2), 269-289.
- Lee, S.Y., Ryu, S.U., 2006. Recent progress of spray-wall interaction research, *Journal of Mechanical Science and Technology*, Vol. 20, 1101-1117.
- Mahulkar, A.V., Heynderickx, G.J., Marin, G.B., 2012, Simulation of Coking in Convection Section of Steam Cracker. 15th International Conference on Process Integration, Modelling and Optimisation for Energy Saving and Pollution Reduction, *Chemical Engineering Transactions*, vol. 29, pp. 1375-1380.
- Mahulkar, A.V., Heynderickx, G.J., Marin, G.B., 2014, Simulation of the Coking Phenomenon in the Superheater of a Steam Cracker, *Chemical Engineering Science*, vol. 110, 31-43.
- Mahulkar, A.V., Marin, G.B., Heynderickx, G.J., 2015, Droplet-wall interaction upon impingement of heavy hydrocarbon droplets on a heated wall, 2015, *Chemical Engineering Science*, vol. 130, , 275-289.
- Mundo, C., Sommerfeld, M., Tropea, C., 1995. Droplet-wall collisions-experimental study on the deformation and break-up process. *Int. J. Multiph. Flow*, 21, 151-173.
- Ogawa, H., Matsui, Y., Kimura S., Kawashima, J., 1997. Three-dimensional computation of in-cylinder flow and combustion characteristics in diesel engines – effect of wall impingement models of fuel droplet behavior on combustion characteristics, *JSAE Review*, vol. 18, 95-99.
- Werner, S., Jones, J., Patterson, A., Archer R., Pearce, D., 2007. Air-suspension coating in the food industry: Part II-micro-level approach. *Powder Technology*, vol. 171, 34-45.
- Wiehe, I.A., 1993, A phase-separation kinetic model for coke formation, *Industrial & Engineering Chemistry Research*, vol. 32, pp. 2447-2454.